Computer Fraud and Security
ISSN (online): 1873-7056

Robust Control of Robot Dexterity Operation Based on Harmony Search Genetic Algorithm

Zhaolan He[1,*], Xingrong Zhu[1], Shuming Jia[2], Cong Xue[3]

[1]*College of Mechanical and Electrical Engineering, Guangdong University of Science and Technology, Dongguan 523083, Guangdong, China*

[2]*State Grid Heilongjiang Electric Power Co., Ltd. Heihe Power Supply Company, Heihe 164300, Heilongjiang, China*

[3]*Department of Control Science and Engineering, Harbin Institute of Technology, Harbin 150001, Heilongjiang, China*

** Corresponding Author.*

Abstract:
In response to the characteristics of multiple variables, uncertain parameters, complex structure, and strong coupling in the agile operation control system of robots, an adaptive genetic algorithm with cross probability and mutation probability is adopted to improve the control rate and steady-state accuracy of the control system. Integrating harmony search algorithm thinking with genetic algorithm to further optimize the parameters of the robot's agile operation controller in the initial population generation process. The simulation has verified that the optimization algorithm can effectively improve the control efficiency, steady-state accuracy, and robustness of the controller, and can ensure that the overshoot value of the system is within an appropriate range.

Keywords: robot dexterous operation, harmony search algorithm, genetic algorithm, robust pid control

INTRODUCTION

The new core components and agile operation of robots are one of the top ten cutting-edge hot topics in robotics released at the 2023 World Robotics Conference. The robotic arm is a key component for achieving agile robot operations and is widely used in manufacturing, medical rehabilitation, service robots, and other fields[1-3], completing operational tasks in complex scenarios. With the increasing demand for robot functionality and performance, higher requirements have been put forward for the stability and effectiveness of robotic arm systems. The control system of robotic arms has the characteristics of high complexity and strong uncertainty, mainly reflected in structural uncertainty and non structural uncertainty[4]. Scholars are committed to finding a perfect control scheme to achieve control of robotic arms. The most commonly used control scheme is the traditional PID controller. In modern control schemes, different modeling methods for robotic arms have different characteristics, so different control methods are needed to control them according to their own characteristics[5]. There are mainly adaptive control methods, variable structure control methods, robust PID control methods, and the evolution or combination of these control methods. To ensure that the parameters of the robot control system can match the dynamic characteristics in real time, Han et al. designed a hybrid fuzzy PID controller for the TriMule robot[6]. At present, the flexibility and stability of robotic arm control can basically meet the requirements of people's daily production and life. But it still cannot adapt well to complex scenarios and task requirements.

The most important feature of genetic algorithm is the use of population search strategy, which emphasizes the information interaction between individuals in the population and is suitable for solving complex nonlinear problems. Therefore, it has been applied in many fields such as combinatorial optimization, artificial intelligence, machine learning, and adaptive control, and has achieved great success. A comprehensive review, research status, and future development trends of genetic algorithms have been conducted, providing useful assistance to researchers in this field[7]. Ayesha Sohail expound the improved genetic algorithms or integration with other algorithms, these algorithms are used in the fields of engineering and information sciences[8]. A genetic algorithm based on upward climbing and multi intelligence algorithm fusion is proposed for medical image tomography[9]. This algorithm can exactly refactoring low-noise CT images in the absence of sufficient effective information. Mahfoud introduced a fault diagnosis method for a doubly fed induction motor, which is powered by two voltage inverters. A PID controller is designed based on genetic algorithm to regulate the engine speed, and the parameters of the PID controller are further adjusted and optimized using a weighted combination method[10].Muhammad

design a domain controller based on the characteristic of the Fuzzy PID parameters, Optimized the PID controller algorithm to improve the accuracy of autonomous demand path planning position and angle[11].

The harmony search algorithm(HSA) was invented by Korean scholar Zong et al., and has been proven to be more efficient in problem-solving than traditional genetic algorithms, particle swarm optimization algorithms, etc. in certain specific environments. In recent years, research on fusion algorithms based on harmony search algorithms and some other algorithms has become a research hotspot[12-15]. The harmony search algorithm, as a type of natural algorithm, has excellent algorithmic thinking, excellent algorithm flow, and excellent algorithm performance. However, its performance in solving certain problems is still lacking. In order to obtain algorithms with better performance, many scholars studying harmony search algorithms have shifted their focus to the combination of harmony search algorithms and genetic algorithms, taking advantage of the strengths of their respective algorithms to make up for their shortcomings. A new fusion algorithm (HACOHS) is developed by integrating ant colony algorithm, harmony search algorithm, and genetic algorithm[16]. This algorithm applies ant colony algorithm and harmony search algorithm to find the global optimal solution. Throughout the entire data processing process, genetic algorithms are applied to the segment selection stages of HACOHS. Traditional genetic algorithm programs run slowly and cannot meet real-time requirements. Therefore, A applies the acoustic search algorithm to select the fitness function of the genetic algorithm, which can greatly improve speed and efficiency[17]. In order to overcome the computational difficulties and long time consuming problems in optimizing parameters, harmony search genetic algorithm (HSGA) is used to optimize the identified model's parameters[18]. The simulation result has proved its correctness. The Smith predictor using harmony search genetic algorithm as a model identification parameters optimization algorithm has greatly improved the stability, effectiveness and even robustness of the time-delay controller.

Based on the research results of the scholars mentioned above, a controller for a 6-degree-of-freedom robotic arm was designed using harmony search genetic algorithm, which improves the control efficiency, steady-state accuracy, and robustness of the controller, meets the performance indicators of robot dexterity operation, and can better adapt to various complex environments and task requirements.

DESIGN OF ROBOTIC ARM CONTROLLER

Kinetic Equation

The dexterity of robot motion mainly depends on the accuracy and robustness of its robotic arm control system. Due to the unique structural characteristics of the robotic arm, the motion pair at the front end and bottom is a single motion pair, while the motion chain between the two ends is composed of a double motion pair member. In the entire robotic arm system, except for the end members, all other intermediate members need to include two motion pairs and two motion axes, so that the joints and the connecting rods at both ends can be connected, and the joints and connecting rods of the robotic arm can work together. The main research content of the kinematics of a robotic arm is the relationship between the overall kinematic equation of the system and various variables and parameters during the motion process of the robotic arm.

The parameters of a robotic arm are defined using the D-H transformation. The total homogeneous transformation matrix T of a robotic arm with six joints from the tail of the hand to the basic coordinates {0} can be expressed as the product of matrix A.

$$T_6 = A_1 A_2 A_3 A_4 A_5 A_6 \tag{1}$$

The homogeneous matrix A is used to represent the correspondence between two connecting rods, and Ai is used to represent the location and posture of the i-th connecting rod relative to the i-1th connecting rod.

For the convenience of calculation, the center of the robotic arm's fingertip is defined as the base point of the desired coordinate system, which is represented by the vector q. The direction of the three unit vectors describing the direction of the gripper is defined as follows: the vector z represents the direction in which the gripper enters the object, and this vector is denoted as the approach vector c; The vector y pointing from one fingertip to another is defined as the direction vector o, which is defined in the specified grip direction; Define the normal vector as the direction verticality to the direction of the o and c vectors, and denote it as η. η can also be represented by the vector product of o and c, whose direction and size are determined by $\eta = o \times c$.

Therefore, the elements in the transformation matrix T_6 from the gripper of the robotic arm to the basic coordinates {0} of the robotic arm can be represented by equation (2). This matrix is composed of the projection of the unit vector of the gripper coordinate system of the robotic arm onto the base coordinate system {0} of the robotic arm, as well as the component of the offset vector between the origin points of these two coordinate systems

$$T_6 = \begin{bmatrix} \vartheta_x & o_x & c_x & q_x \\ \vartheta_y & o_y & c_y & q_y \\ \vartheta_z & o_z & c_z & q_z \\ 0 & 0 & 0 & 1 \end{bmatrix} \tag{2}$$

The values of each parameter are:

$$\vartheta_x = B_1(B_{23}B_4B_5B_6 - \Xi_{23}\Xi_5B_6 + B_{23}B_4B_6) + \Xi_1(\Xi_4B_5B_6 + B_4\Xi_6)$$

$$\vartheta_y = \Xi_1(B_{23}B_4B_5B_6 - \Xi_{23}\Xi_5B_6 + B_{23}B_4B_6) - B_1(\Xi_4B_5B_6 + B_4\Xi_6)$$

$$\vartheta_z = -\Xi_{23}(B_4B_5 + \Xi_4\Xi_6) - B_{23}\Xi_5B_6$$

$$O_x = B_1(-B_{23}B_4B_5B_6 + \Xi_{23}\Xi_5\Xi_6 + B_{23}\Xi_4B_6) + \Xi_1(-\Xi_4B_5B_6 + B_4\Xi_6)$$

$$O_y = \Xi_1(-B_{23}B_4B_5B_6 + \Xi_{23}\Xi_5\Xi_6 + B_{23}\Xi_4B_6) - B_1(-\Xi_4B_5B_6 + B_4\Xi_6)$$

$$O_z = \Xi_{23}(B_4B_5B_6 - \Xi_4\Xi_6) + B_{23}\Xi_5\Xi_6$$

$$c_x = B_1(-B_{23}B_4\Xi_5 - \Xi_{23}B_5) - \Xi_1\Xi_4\Xi_5$$

$$c_y = \Xi_1(-B_{23}B_4\Xi_5 - \Xi_{23}B_5) + B_1\Xi_4\Xi_5$$

$$c_z = \Xi_{23}B_4\Xi_5 - B_{23}B_5$$

$$q_x = B_1(B_{23}c_3 - \Xi_{23}d_4 + B_2c_2 + c_1)$$

$$q_y = \Xi_1(B_{23}c_3 - \Xi_{23}d_4 + B_2c_2 + c_1)$$

$$q_z = -\Xi_{23}c_3 - B_{23}d_4 - \Xi_2c_2$$

In the above equation, Ξ_i represents $\sin\beta_i$ and B_i represents $\cos\beta_i$, $\Xi_{ij} = \sin(\beta_i + \beta_j)$.

T_6 represents the total transformation matrix of the 6-degree of freedom(DOF) robot arm, which is the obtained pose motion equation of the robot arm. In fact, this equation explains the pose of the end link coordinate system {6} relative to the coordinate system {0}. The matrix transformation here includes rotation, movement, etc.

The kinetic equation of the robotic arm can be expressed by equation (3) through matrix transformation using the Lagrange equation

$$M(\rho)\ddot{\rho} + C(\rho,\dot{\rho})\dot{\rho} + g(\rho) = \tau \tag{3}$$

Among them, ρ, $\dot{\rho}$, $\ddot{\rho}$ represents the joint position, velocity, and acceleration vector of the robotic arm, and $M(\rho)$ represents the positive definite inertia matrix of the robotic arm. $B(\rho,\dot{\rho})$ represents the centrifugal force and Coriolis force matrix of the system. $g(\rho)=\partial U(\rho)/\partial\rho$ represents the gravitational vector. $U(\rho)$ is the potential energy caused by gravity. τ represents the force/torque vector applied by the external environment to the joint of the robotic arm

For the nonlinear robotic arm system represented by equation (3), it generally has the following structural properties.

Characteristic 1: The inertia matrix $M(\rho)$ is symmetric, positive definite, and bounded.

$$0 \le \lambda_m(M) \le \|M(\rho)\| \le \lambda_M(M) \tag{4}$$

Characteristic 2: The Coriolis force and centrifugal force matrix $B(\rho,\dot{\rho})$ have the relationship.

$$B(\rho,\xi)v = B(\rho,v)\xi \qquad \forall \rho,\xi,v \in R^n \tag{5}$$

$$0 < B_m \|\dot{\rho}\|^2 \le \|B(\rho,\dot{\rho})\dot{\rho}\| \le B_M \|\dot{\rho}\|^2 \qquad \forall \rho,\dot{\rho} \in R^n \tag{6}$$

Where B_M and B_m are normal numbers.

Characteristic 3: $\dot{M}(\rho) - 2B(\rho,\dot{\rho})$ is an antisymmetric matrix, i.e

$$\zeta^T(\dot{M}(\rho) - 2B(\rho,\dot{\rho}))\zeta = 0 \qquad \forall \zeta \in R^n \tag{7}$$

Characteristic 4: For a specific ρ_d and any ρ and $c > 0$, there exists a constant diagonal positive definite matrix A that can hold the two equations below.

$$U(\rho) - U(\rho_d) - \tilde{\rho}^T g(\rho_d) + \frac{1}{2}\tilde{\rho}^T A \tilde{\rho} \ge c\|\tilde{\rho}\|^2 \tag{8}$$

$$\tilde{\rho}^T[g(\rho) - g(\rho_d)] + \tilde{\rho}^T A \tilde{\rho} \ge c\|\tilde{\rho}\|^2 \tag{9}$$

Where $\tilde{\rho} = \rho - \rho_d$ is the joint error, ρ_d and ρ are the expected and actual joint positions, respectively.

Characteristic 5: Gravity vector A is bounded.

$$\|g(\rho)\| \le k_g \qquad \forall \rho \in R^n \tag{10}$$

Alternatively, any component of the gravity vector of the robotic arm system satisfies the following equation.

$$\sup_{\rho \in R^n}\{|g(\rho)|\} \le k_{gi} \qquad \forall i = 1,2,\cdots,n \tag{11}$$

Where k_g and k_{gi} are normal numbers.

Controller Design

Consider the following control model.

$$\tau = -(K_{q0} + K_i)\tilde{\rho} - K_i \int_0^t \tilde{\rho}(\sigma)d\sigma - K_d\dot{\rho} \tag{12}$$

Among them, $K_{q0} + K_i$, K_i, K_d represents proportion, integral, and differential gain matrices in the controller, respectively.

$$z(t) = \tilde{\rho} - \int_0^t \tilde{\rho}(\sigma)d\sigma - K_i^{-1}g(\rho_d) \tag{13}$$

Combining equations (12), (13) and (3), the equation of the control loop of the robotic arm can be obtained as

$$M(\rho)\ddot{\rho} + B(\rho,\dot{\rho})\dot{\rho} + g(\rho) - g(\rho_d) + K_{q0}\tilde{\rho} + K_i z + K_d\dot{\rho} = 0 \tag{14}$$

From equation (14), it can be obtained that $\left[\tilde{\rho}^T \dot{\rho}^T z^T\right]^T = 0 \in R^{3n}$ is the unique static equilibrium point of the closed-loop system.

Define the following Lyapunov function.

$$V = \frac{1}{2}\dot{\rho}^T M(\rho)\dot{\rho} + U(\rho) - U(\rho_d) - \tilde{\rho}^T g(\rho_d) - \tilde{\rho}^T M(\rho)\dot{\rho} + \frac{1}{2}\tilde{\rho}^T(K_{q0} + K_d)\tilde{\rho} + \frac{1}{2}z^T K_i z \tag{15}$$

Select the gain matrix K_{q0} based on feature 4, and for any given small enough normal number a, ensure that both equations hold simultaneously.

$$U(\rho)-U(\rho_d)-\Box\rho^T g(\rho_d)+\frac{1}{2}\Box\rho^T K_{q0}\Box\rho\geq c\left\|\Box\rho\right\|^2 \tag{16}$$

$$\Box\rho^T[g(\rho)-g(\rho_d)]+\Box\rho^T K_{q0}\Box\rho\geq c\left\|\Box\rho\right\|^2 \tag{17}$$

From feature 1, it can be selected that the differential gain matrix K_d is sufficiently large, such that

$$K_d-2M(\rho)>0 \tag{18}$$

$$K_d-M(\rho)-\varepsilon C_M I>0 \tag{19}$$

Where ε is a normal number and satisfies $\left\|\Box\rho\right\|\leq\varepsilon$

Lyapunov function (15) takes the derivative of time along system(14)

$$\begin{aligned}\dot{V}=&\dot{\rho}^T M(\rho)\ddot{\rho}+\frac{1}{2}\dot{\rho}^T\dot{M}(\rho)\dot{\rho}+\dot{\rho}^T g(\rho)-\Box\dot{\rho}^T g(\rho_d)+\Box\dot{\rho}^T(K_{q0}+K_d)\Box\rho\\&+\Box\dot{\rho}^T M(\rho)\dot{\rho}+\Box\rho^T\dot{M}(\rho)\dot{\rho}+\Box\rho^T M(\rho)\ddot{\rho}+\dot{z}^T K_i z\end{aligned} \tag{20}$$

Substitute $M(\rho)\ddot{\rho}$ obtained from equation (14) and $\dot{z}=\dot{\rho}+\Box\rho$ obtained from equation (13) into equation (20), and apply feature 3 to obtain

$$\dot{V}=-\dot{\rho}^T[K_d-M(\rho)]\dot{\rho}+\Box\rho^T C^T(\rho,\dot{\rho})\dot{\rho}-\Box\rho^T[g(\rho)-g(\rho_d)+K_{q0}\Box\rho] \tag{21}$$

If feature 2 is applied, there are

$$\Box\rho^T B^T(\rho,\dot{\rho})\dot{\rho}\leq\varepsilon C_m\left\|\dot{\rho}\right\|^2 \tag{22}$$

Substituting equations (17) and (22) into equation (21) yields

$$\dot{V}\leq-\dot{\rho}^T[K_d-M(\rho)-\varepsilon C_M I]\dot{\rho}-c\left\|\Box\rho\right\|^2 \tag{23}$$

From equation (19) and a being normal numbers greater than zero, it can be concluded that $\dot{V}\leq 0$ .It can be inferred from this that the designed control system is stable

In actual control engineering, there may be some errors between the actual object and the nominal model, which are represented by $l(s)$, i.e

$$\left|\frac{P(\eta)-\hat{P}(\eta)}{\hat{P}(\eta)}P(\eta)\right|<l(\eta),\forall\eta \tag{24}$$

When the transfer function of a closed-loop system

$$W(s)=\frac{P(s)C(s)}{1+P(s)C(s)} \tag{25}$$

$\left\|W(\eta)l(\eta)\right\|_\infty<1,\forall\eta$ is satisfied, the system has robustness.

Select equation (26) as the optimal indicator function for the controller.

$$J=\int_0^\infty\left[\eta_1\left|e(t)\right|+\eta_2u^2(t)dt+\eta_3t_u+\eta_4\delta(\sigma)\right] \tag{26}$$

Among them, $e(t)=r(t)-y(t)$ is the system error, $u(t)$ is the controller output, t_u is the rise time, and η_1, η_2, η_3, η_4 are the weights. η_4 η_2. Define the energy term σ function as

$$\delta(\sigma)=\begin{cases}1 & \sigma>5\% \\ 0 & \sigma\le 5\%\end{cases} \tag{27}$$

CONTROLLER PARAMETER OPTIMIZATION

Integration of Harmony Search and Genetic Algorithm

Applying the HSA to the process of generating the initial population of genetic algorithms and improving it to ensure the ability of the control system to maintain stability in the worst-case scenario. The calculation steps of this algorithm are described.

Parameter determination and representation

Determine the parameters that need to be optimized and their range of variation based on the controller characteristics and computational capabilities of the robotic arm. Then, based on the accuracy, binary encoding is performed on the parameters in the selected initial population. Treating each individual as an independent chromosome, as traditional controllers mainly have three parameters, each chromosome is represented by a matrix as

$$E(a)=(a_q,a_I,a_D) \tag{28}$$

Initialize algorithm parameters

Do not select fixed values for mutation and crossover probabilities, and use adaptive methods to control the values of probabilities. To achieve real-time control, flexible control, and efficient control effects.

Set fitness function

The fitness function is the majorization criterion of GA. The larger the fitness value, the higher the possibility of an individual being selected during the selection process. The fitness function is represented as $\psi(a)$.

Initialize population

In order to improve the dispersion and equidistribution of the initial population, an optimization of the HSA is performed on the initial population when selecting individuals. Determine the size of the harmony library as Ξ_{HM}, randomly generate Ξ_{HM} initial harmonies, and store them in the memory library M_H.

code

Encode the harmony library M_H generated by the HSA in binary and connect the beginning and end to form an encoding string, represented by $E(a_1)=(a_1^1,\cdots,a_1^n)$, with each encoding string length set to L.

Harmony

Choose a new solution in M_H with a harmony selection probability P_{HMCR}, randomly select a new individual in the search database with a probability $1-P_{HMCR}$, then locally perturb the tone with a probability P_{PAR}, and finally substitute the generated new solution into the objective function. Based on the value of the objective function, determine whether the new individual is better than the worst individual in M_H. If so, replace it; otherwise, repeat steps (1) to (6) until the termination condition is reached [19]. The M_H initialization process is

$$a_i^j=a_i^L+Random(0,1)(a_i^U-a_i^L) \tag{29}$$

Among them, a_i^j is the decision variable a_i^U, a_i^L represents the maximum and minimum values of the *i*-th dimensional variable, respectively; *j*=1,2,...; $Random(0,1)$ is a random number between 0 and 1.

Generating a new individual is called extemporaneously performance, which uses the P_{HMCR} parameter.

$$a_i^j = \begin{cases} a_i^j \in \{a_i^1, \cdots, a_i^{S_{HM}}\} p = P_{HMCR} \\ a_i^j \in X_i \qquad p = 1 - P_{HMCR} \end{cases} \tag{30}$$

Where p is a random probability.

After selection, each individual needs to make a certain judgment to determine whether they need to undergo pitch adjustment. This operation uses parameter P_{PAR} .

$$a_i^j = \begin{cases} a_i^j \pm Random(0,1) b_w \quad p = P_{PAR} \\ a_{i\,i}^{\,j} \qquad\qquad\qquad\qquad p = 1 - P_{PAR} \end{cases} \tag{31}$$

Among them, b_w is the step size for tone adjustment.

Select

Randomly select individuals from the encoded individuals for genetic manipulation. The percentage of individual *a* being selected is $\frac{\psi(a)}{\sum \psi(a)}$, $\sum \psi(a)$ is the total fitness value of the population.

Cross

Adopting an adaptive crossover probability selection strategy, where the crossover probability is

$$P_c = \begin{cases} \dfrac{K_1(\psi_{\max} - \psi')}{f_{\max} - f_{avg}}, \psi' > \psi_{avg} \\ K_{2,}\psi' < \psi_{avg} \end{cases} \tag{32}$$

Among them, P_c is the crossover probability, $\psi_{\max}$ is the maximum fitness value in the present population, ψ' is the large one between two individuals undergoing crossover, and ψ_{avg} is the average fitness value in the present population.

Mutation

Applying the adaptive concept to select mutation probability, i.e. the mutation probability is

$$P_m = \begin{cases} \dfrac{K_3(\psi_{\max} - \psi')}{\psi_{\max} - \psi_{avg}}, \psi' > \psi_{avg} \\ K_{4,}\psi' < \psi_{avg} \end{cases} \tag{33}$$

Here P_m is the mutation probability. Everything else is the same as the above equation.

Decoding

Repeat steps(7) to (9) until the most times of iterations is reached. Generate the final harmony library HS. Output majorization results, decode, and obtain the majorization solution $E(a_{BEST}) = (a_{BEST}^1, \cdots, a_{BEST}^n)$.

Optimize Controller Parameters

The design diagram of a robotic arm control system based on improved HSGA optimization is shown in Figure 1. Among them, $r(t)$ is the controller input, $u(t)$ is the controller output, and $y(t)$ is the actual output of the controlled robotic arm.

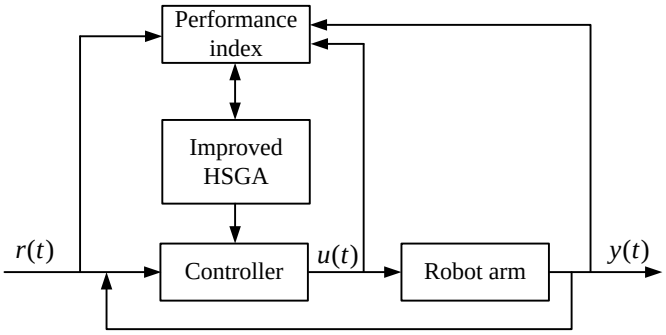

Figure1. The block diagram of robust control system based on improved HSGA

Apply the improved HSGA to the solution process of the optimal control parameter $E(a_{BEST}) = E(a_{BEST}^{P}, a_{BEST}^{I}, a_{BEST}^{D})$ of the robust controller for a robotic arm. The solving process involves the following four steps.

Parameter determination and representation

Based on experience, set the size of the selected harmony memory library to M within the range of K_P, K_I, K_D. After confirmation, use decimal encoding to encode all items in the harmony memory library. According to equation (28), each chromosome is represented by a matrix for $E(a) = (a_P, a_I, a_D)$.

Determine the size of the harmony pool Ξ_{HM}, the probability of harmony selection P_{HMCR}, the probability of pitch adjustment P_{PAR}, the number of harmony adjustments N_1, the number of genetic operations N_2, the probability of genetic selection P_{GA}, the probability of genetic crossover P_c, and the probability of genetic variation P_m.

Determination of fitness function

The closed-loop equation, objective function, and penalty function of the control loop of the robotic arm are Equation (14), Equation (26), and Equation (27), respectively.

The selection criteria for parameters η_1, η_2, η_3, η_4 are as follows.

① Firstly, keep the numerical values of each goal function term on the equual level of magnitude to ensure that the impact of each term on the goal function is averaged.

② Adjust the weights of each item accordingly based on the results.

Calling the Harmony Search Genetic Algorithm Function for Calculation

Select a new solution in the Harmony Memory Library (HM) with probability P_{HMCR}, and select a new individual in the primitive search library with probability $1-P_{HMCR}$. The selected new solution is represented as $E_0(a) = (a_{P0}, a_{I0}, a_{D0})$ as the data processed by the current algorithm.

Adjust the pitch of the selected solution with a probability of P_{PAR}, resulting in a new solution $E_1(a) = (a_{P1}, a_{I1}, a_{D1})$.

Call the degree function J to calculate the new individual. If it performs better than the worst individual in HM, replace the worst solution with the new individual and proceed to the next cycle. If the performance of the new individual is not better than the worst solution in HM, discard the individual and proceed directly to the next cycle.

Until N_1 harmonic operations are performed, a new N_1 generation solution is generated, and after evaluating its fitness, a new HM is generated. Use HM as the initial population for genetic operations.

Select individuals as genetic operators in HM using the selection probability P_{GA}, and represent it as $E_{N_1}^0(a) = (a_{PN_1}^0, a_{IN_1}^0, a_{DN_1}^0)$.

Determine whether to perform crossover and mutation operations on the selected individual $E_{N_1}^0(a)=(a_{PN_1}^0,a_{IN_1}^0,a_{DN_1}^0)$ based on P_c and P_m. P_c and P_m are shown in equations (32) and (33).

After performing a genetic operation, a new solution $E_{N_1}^1(a)=(a_{PN_1}^1,a_{IN_1}^1,a_{DN_1}^1)$ is obtained, and the fitness of the new individual is calculated based on the fitness function J.

Perform the next genetic operation until the maximum genetic operation algebra N_2 is reached, resulting in a new solution $E_{N_1}^{N_2}(a)=(a_{PN_1}^{N_2},a_{IN_1}^{N_2},a_{DN_1}^{N_2})$. At this point, a new HM has been generated.

Select the individual $E_{BEST}(a)=(a_{PBEST},a_{IBEST},a_{DBEST})$ in HM that best meets the fitness requirements and decode it.

Optimizing controllers

Select the optimal parameters obtained in step (3) to perform real-time control on the robust controller of the robotic arm. Obtain overall control data of the system.

SYSTEM SIMULATION

Improve Algorithm Performance Testing

Performance indicator testing

Based on the actual characteristics of the algorithm, the maximum, minimum, average, and standard deviation of the convergence index GD, diversity index Δ, and dispersion index SP, which are used to evaluate the effectiveness of the algorithm, are determined.

Set the overall evolution generation of the algorithm to 300, with 100 iterations for harmony adjustment and 200 iterations for genetic operation. Set the iteration count of the improved genetic algorithm to 300. Test the functions belegondu, binh, srinivas, and tanaka 20 times for each algorithm. The expressions for belegundu, binh, srinivas, and tanaka are shown in equations (34) to (37), respectively. Obtain the statistical results shown in Tables 1 to 4.

$$\begin{cases} \min \psi_1(\chi,\gamma) = -2\chi+\gamma \\ \min \psi_2(\chi,\gamma) = 2\chi+\gamma \\ s.t. \quad -\chi+\gamma-1\le 0 \\ \chi+\gamma-7\le 0 \end{cases} \tag{34}$$

Here $0\le\chi\le 5, 0\le\gamma\le 3$

$$\begin{cases} \min \psi_1(\chi,\gamma) = 4\chi^2+4\gamma^2 \\ \min \psi_2(\chi,\gamma) = (\chi-5)^2+(\gamma-5)^2 \\ s.t. \quad (\chi-5)^2+\gamma^2-25\le 0 \\ -(\chi-8)^2-(\gamma-3)^2+7.7\le 0 \end{cases} \tag{35}$$

Here $-15\le\chi,\gamma\le 30$

$$\begin{cases} \min \psi_1(\chi,\gamma) = (\chi-2)^2+(\gamma-1)^2+2 \\ \min \psi_2(\chi,\gamma) = 9\chi-(\gamma-1)^2 \\ s.t. \quad \chi^2+\gamma^2-225\le 0 \\ \chi-3\gamma+10\le 0 \end{cases} \tag{36}$$

Here $-20\le\chi,\gamma\le 20$

$$\begin{cases} \min \psi_1(\chi,\gamma) = \chi \\ \min \psi_2(\chi,\gamma) = \gamma \\ s.t. \quad -\chi^2 - \gamma^2 + 1 - 0.1 * \cos(16 \arctan \frac{\chi}{\gamma}) \le 0 \\ (\chi - \frac{1}{2})^2 + (\gamma - \frac{1}{2})^2 - \frac{1}{2} \le 0 \end{cases} \tag{37}$$

Here $0 \le \chi, \gamma \le pi$

From Tables 1 to 4, it can be seen that for the four test functions, the convergence and dispersion of the improved harmony search genetic algorithm in this paper are significantly better than those of the improved genetic algorithm. In terms of diversity, for functions binh and srinivas, the HSGA method is better than GA, and for functions belegondu and tanaka, the HSGA method is more stable than GA.

Table 1. The statistical results of evaluation criteria of belegundu

evaluating	GD		Δ		SP	
algorithm	GA	HSGA	GA	HSGA	GA	HSGA
Maximum value	0.0190	9.200e-004	1.6219	1.6010	0.0158	0.0018
minimum value	0.0025	9.6800e-005	1.1480	0.8990	0.0050	1.0000e-004
average value	0.0095	1.7367e-004	1.3419	1.0693	0.0095	5.6000e-004
standard deviation	0.0048	2.0721e-004	0.1211	0.1998	0.0029	5.8560e-004

Table 2. The statistical results of evaluation criteria of binh

evaluating	GD		Δ		SP	
algorithm	GA	HSGA	GA	HSGA	GA	HSGA
Maximum value	0.0907	0.0367	1.2986	0.9745	0.2921	0.1157
minimum value	0.0205	0.0079	1.0527	0.6546	0.0511	0.0029
average value	0.0325	0.0139	1.1675	0.7762	0.1328	0.0331
standard deviation	0.0169	0.0074	0.0821	0.1131	0.0681	0.0335

Table 3. The statistical results of evaluation criteria of srinivas

evaluating	GD		Δ		SP	
algorithm	GA	HSGA	GA	HSGA	GA	HSGA
Maximum value	0.1362	0.0060	1.2443	0.6607	0.3171	0.0351
minimum value	0.0215	0.0026	1.0539	0.5886	0.0845	0.0115
average value	0.0708	0.0037	1.1197	0.6188	0.1486	0.0171
standard deviation	0.0297	8.3512e-004	0.0582	0.0222	0.0534	0.0065

Table 4. The statistical results of evaluation criteria of tanaka

evaluating	GD		Δ		SP	
algorithm	GA	HSGA	GA	HSGA	GA	HSGA
Maximum value	0.0032	0.0024	1.3633	1.2264	0.0120	0.0062
minimum value	1.6695e-004	3.0000e-004	1.0341	0.9672	2.1437e-004	4.0000e-004
average value	9.5232e-004	7.5333e-004	1.1689	1.0225	0.0029	0.0010
standard deviation	7.8863e-004	6.0694e-004	0.0981	0.0669	0.0032	0.0014

Optimization algorithm efficiency testing

Choose two representative functions as instance functions to verify algorithm performance.

Find the global maximum value of the Schaffer function and the Needle in a haystack function. The expressions for these two functions are shown in equations (38) and (39).

$$\psi(\chi_1,\chi_2)=0.5-\frac{\sin^2\sqrt{\chi_1^2+\chi_2^2}-0.5}{[1+0.001(\chi_1^2+\varphi_2^2)]^2}(-100\le\chi_i\le100) \tag{38}$$

$$\psi(\varphi,\gamma)=\left[\frac{3}{0.05+(\chi^2+\gamma^2)}\right]^2+(\chi^2+\gamma^2)\qquad(-5.12\le\chi,\gamma\le5.12) \tag{39}$$

The parameter settings for calculating the maximum value of the Schaffer function using GA are defined as: group size M=50, termination iteration count T=500, crossover odds $P_c=0.8$, and mutation odds $P_m=0.1$. When the algorithm evolved to the 305 generation, the function found the optimal approximate solution of 0.990284 for this solution.

The parameter settings for the HSGA are: the size of the harmony memory library is defined as M=50, the number of harmony iterations is $T_1=200$, and the number of iterations for the genetic part is $T_2=300$. The adaptive mutation probability and adaptive crossover probability are determined by default values. When the algorithm iterates to the 245th generation, the value of the independent variable is 0.9987602.

The evolution process results that two algorithms solve for the maximum value of the Schaffer function are shown in Figure 2.

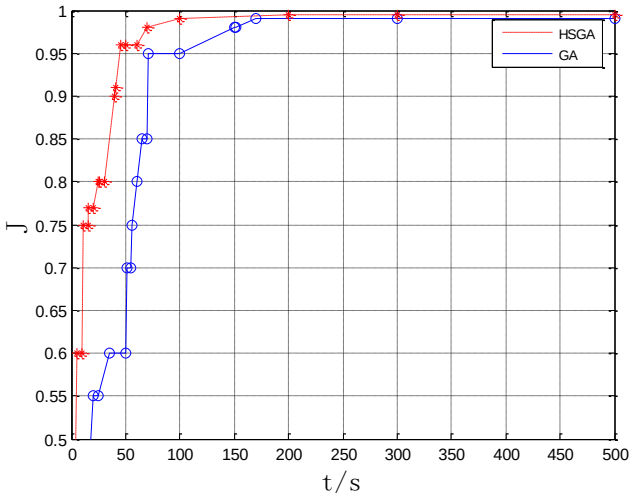

Figure 2. Running chart of Schaffer function algorithm

The parameter settings for improving the GA to solve the maximum value of the Needle in a haystack function are: population size M=80, termination algebra T=100, crossover odds $P_c=0.8$, mutation odds $P_m=0.05$. When the algorithm evolves to the 92nd generation, the fitness function reaches its maximum value, and the function finds the optimal approximate solution 3496.734959 for this solution.

The parameter settings for the HSGA are: the size of the harmony memory library M=80, the number of harmony iterations $T_1=50$, and the number of iterations for the genetic part $T_2=50$. The adaptive mutation probability and adaptive crossover probability are determined by default values. When iterating to the 53rd generation, a peak appeared, followed by a peak that continued until the 58th generation. The next peak appeared in the 88th generation, and the peak continued until the end. The optimal approximate solution for this solution, 3563.785955, was found. The evolution process and operation results of two algorithms for solving the maximum value of the Needle - in - a -haystack function are shown in Figure 3.

Two types of functions were tested 500 times using improved GA and improved HSGA, and the time taken to get the optimal solution was statistically analyzed as Table 5.

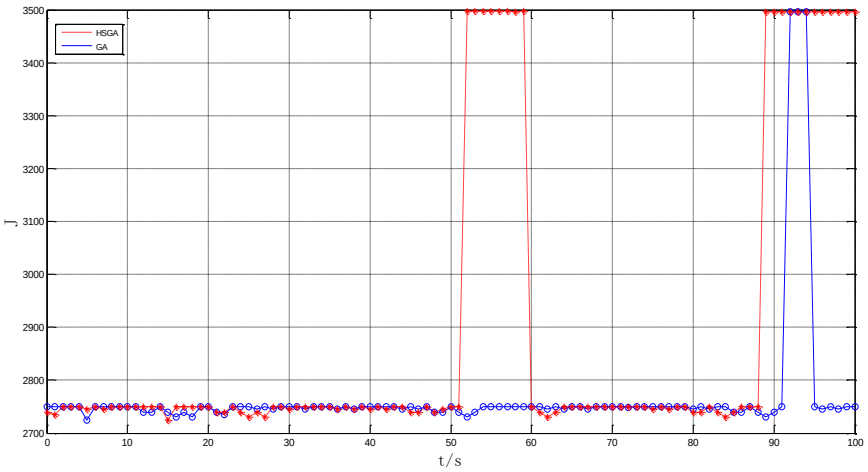

Figure 3. Running chart of Needle - in - a - haystack function algorithm

From the evolution process results of the two examples in Figure 2 and Figure 3, it can be seen that the search speed of the Harmony Search Genetic Algorithm is higher than that of the Improved Genetic Algorithm. When solving the optimal solution of the Needle - in - a - haystack function in the test function, the Harmony Search Genetic Algorithm has already searched for the optimal solution in the 52nd generation and continued until the 60th generation. Due to the superiority of the algorithm, after the 60th generation, the algorithm tends towards suboptimal solutions. Prevent the generation of local optimal solutions from affecting the calculation results.

Controller Performance Testing

Initialize parameters

Based on the characteristics of the robotic arm controller and the research experience of previous scholars, we have chosen an optimization space of $K_P \in [0,20]$, $K_I \in [0, 30]$, $K_D \in [0,20]$ and set the accuracy to ε=0.001. The optimization index parameters are $\eta_1 = 0.999$, $\eta_2 = 0.001$, $\eta_3 = 100$, $\eta_4 = 2$ respectively.

Define the size of the selected harmony memory library to 100 and the number of iterations for the harmony operation to 100. The number of iterations for the genetic algorithm operation is selected as 200. The crossover odds and mutation odds of genetic operations are both using adaptive methods. Based on experience, the probability of selecting harmony and adjusting pitch are 0.68 and 0.55, respectively.

Simulation results

Using the HSGA to majorize the controller parameters, the initial size of the harmony memory library is selected as 100, the number of iterations for the harmony operation is 100, and the number of iterations for the later genetic operation is 200. The other parameters have the same definition as above. The variation curve of the system optimal indicators function J obtained is shown in Figure 4, and the system step response curve is shown in Figure 5.

The robust controller of the robotic arm was optimized using HSGA, and the controller control effect obtained is shown in Table 5.

Comparing the simulation results of the controller optimized by the improved genetic algorithm with the controller optimized by the improved HSGA, results shown that the controller optimized by the new algorithm has significant improvements in stability time, overshoot, steady-state accuracy, and other aspects. When external disturbances are introduced, the robotic arm controller optimized by HSGA also exhibits good robustness. From the response curves of the six joints, it can be seen that the improved HSGA is much higher than the improved GA in terms of speed in obtaining the optimal indicators. In terms of handling step response, improving the HSGA can respond more quickly and the system more stablility.

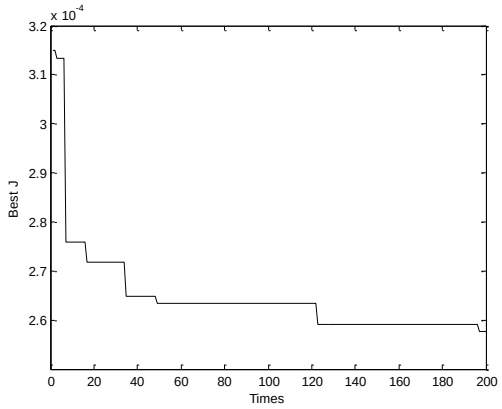

Figure 4. The change of optimization function J

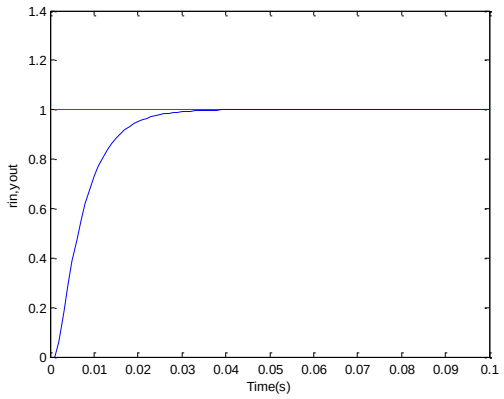

Figure 5. The system step response curve

Applying the HSA to the process of generating the initial population of genetic algorithms and improving it to ensure the ability of the control system to maintain stability in the worst-case scenario. The calculation steps of this algorithm are described.

Table 5. Each joint control performance under improved HSGA

Control methods	Joint number	Adjusting time t(s)	overshoot $\sigma\%$	Metastable precision $e(^\circ)$
A Robust Controller Based on Improved HSGA	1	2.250	0.05%	0.001
	2	1.658	0.02%	0.003
	3	0.250	0.10%	0.001
	4	0.980	0.03%	0.002
	5	0.750	0.09%	0.009
	6	1.860	0.08%	0.002

CONCLUSION

Aiming at the problems of insufficient control accuracy, low control efficiency, and insufficient control stability in traditional robotic arm control schemes, the optimization algorithm problem of robotic arm control was studied. The genetic algorithm and harmony search algorithm were improved, and the two were organically combined to optimize the parameters of the robotic arm controller. MATLAB simulation has verified that the improved optimization scheme proposed in this paper can improve the regulation efficiency, steady-state accuracy, robustness, system overshoot, and response speed to disturbances of the robotic arm control system to a certain extent. It can better complete agile operation tasks in various complex scenarios.

ACKNOWLEDGMENTS

This research was supported by National Natural Science Foundation of China funding project (62173107,U23A20346); Guangdong University of Science and Technology Doctoral Initiation Fund Project (GKY-2023BSQD-50).

REFRENCES

[1] Suhas Kadalagere Sampath, Ning Wang, Hao Wu, et al. Review on human like robot manipulation using dexterous hands, Cognitive Computation and Systems, 2023, 5(1): 14-29.
[2] Isidore Komofor Ngongiah, Ramakrishnan Balamurali, Gaetan Fautso Kuiate, etal. Mechanical arm(s) driven by Josephson junction circuit(s), mimicking the movement pattern of myriapods, Physica Scripta, 2023, 98(4):1-14.
[3] Mcdowell T W, Welcome D E, Warren C, et al. The Effect of a Mechanical Arm System on Portable Grinder Vibration Emissions. The Annals of Occupational Hygiene, 2016(3):240-245.
[4] Kai A N, Wang F. Sliding mode variable structure control for flexible joint of single connecting-rod mechanical arm. Modern Electronics Technique,2016:120-125.
[5] Cosimo Della Santina, Christian Duriez, Daniela Rus, Model-Based Control of Soft Robots: A Survey of the State of the Art and Open Challenges, IEEE Control Systems Magazine, 2023, 43(3): 30-65.
[6] Jiale Han, Xiaolei Shan, Ning Wang, et al. Fuzzy gain scheduling PID control of a hybrid robot based on dynamic characteristics, Mechanism and Machine Theory, 2023, 184(6): 105283.
[7] Sourabh Katoch, Sumit Singh Chauhan, Vijay Kumar, review on genetic algorithm: past, present, and future, Soft Computing, 2021, (80): 8091-8126.
[8] Ayesha Sohail, Genetic Algorithms in the Fields of Artificial Intelligence and Data Sciences, AI in Civil Engineering, 2023, (10): 1007-1018.
[9] Raghavendra Mishra, Manish Kumar Bajpai, A novel multi-agent genetic algorithm for limited-view computed tomography, Expert Systems with Applications, 2024, 238(3): 122195.
[10] Said Mahfoud, Aziz Derouich, Najib EL Ouanjli, et al. A New Strategy-Based PID Controller Optimized by Genetic Algorithm for DTC of the Doubly Fed Induction Motor, Systems, 2021, 9(2): 37-46.
[11] Muhammad Razmi Razali, Ahmad Athif Mohd Faudzi, Abu Ubaidah Shamsudin. A hybrid controller method with genetic algorithm optimization to measure position and angular for mobile robot motion control, Frontiers in Robotics and AI, 2023, 9(1): 1-14.
[12] Ghiduk Ahmed S, Alharbi Abdullah. Generating of Test Data by Harmony Search Against Genetic Algorithms, Intelligent Automation and Soft Computing, 2023, 36(1): 647.
[13] Ghiduk Ahmed S, Alharbi Abdullah. Generating of Test Data by Harmony Search Against Genetic Algorithms, Intelligent Automation and Soft Computing, 2023, 36(1): 647.
[14] Jagatheesan K, Anand B, Samanta S, et al. Design of a proportional-integral-derivative controller for an automatic generation control of multi-area power thermal systems using firefly algorithm. IEEE/CAA J Autom Sin, 2019, 6(2):503–515.
[15] Hameed, F. A., Tariq, K. R., Hasan, H. R., & Johni, R. A. (2024). Using the Cuckoo Optimization to Initialize the Harmony Memory in Harmony Search Algorithm to Find New Hybrid (CSHS) Algorithm. UHD Journal of Science and Technology, 2024, 8(1), 99–107.
[16] Talebpour M H, Kaveh A, Kalatjari V R. Optimization of skeletal structures using a hybridized ant colony-harmony search-genetic algorithm. Iranian Journal of Science and Technology - Transactions of Civil Engineering, 2014, 38(C1):1-20.
[17] Mao C. Harmony search-based test data generation for branch coverage in software structural testing. Neural Computing and Applications, 2014, 25(1):199-216.
[18] Zongze Liu, Lingshan Kong, Chun Fan, et al. Time-Delay System Identification Based on Harmony Search Genetic Algorithm, 2023 China Automation Congress (CAC),17-19 November 2023.
[19] Katal N., Singh S. K.. Multi-objective optimisation of PID controller for DC servo motor using genetic algorithm. Engineering Intelligent Systems, 2015, 23(1): 7-16.